Report of SCEC Project **#19238**

Multi-cycle Dynamics of the San Andreas and San Jacinto Faults in Southern California

Principle Investigator: **Benchun Duan (TAMU)**

Deciphering and understanding rupture behaviors of the San Andreas and San Jacinto faults are among the most important goals of seismic hazard assessment in Southern California. Dynamic rupture models on realistic fault geometries in the context of earthquake cycles is one of physics-based tools to address the issue. The Cajon Pass, which is the triple junction between the San Andreas and San Jacinto faults, and the Big Bend on the San Andreas fault are two prominent fault geometrical complexities, i.e., earthquake gates, that influence earthquake rupture extents and magnitudes of earthquakes. In this project, we explore multicycle dynamics of the San Andreas fault from Parkfield to Salton Sea and the San Jacinto Fault (Claremont segment) with our 2D numerical methods for earthquake cycles. The method consists of a finite element model for coseismic spontaneous ruptures and an analytic Maxwell viscoelastic model representing the tectonic loading, viscoelastic relaxation and off-fault deformation (Duan and Oglesby, 2005; Duan, 2019; Duan *et al.*, 2019). We adopt realistic fault geometry from the Community Fault Model 5.2 (Plesch *et al.*, 2007, Nicholson *et al.*, 2017) for our models. The fault geometric complexity is the only heterogeneity we consider in the models while we keep the shear loading uniform. Figure 1 shows fault geometries and the maximum shearing direction used in the project.

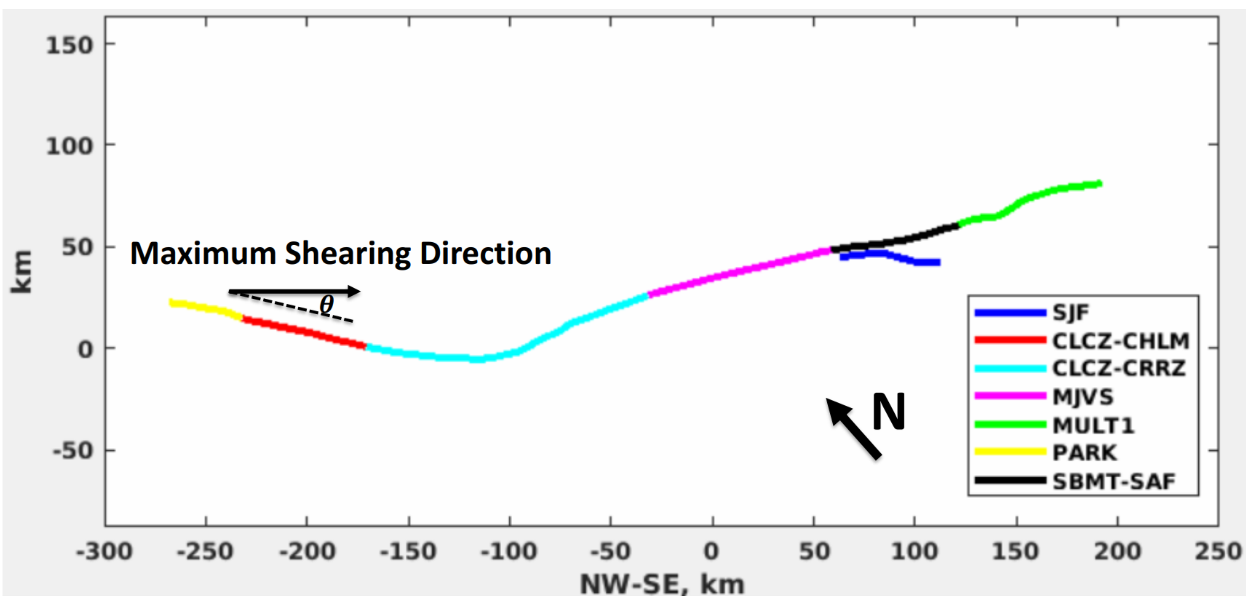

Figure 1. Geometries of the San Andreas and San Jacinto faults simulated in the project. The controlling points of fault geometries are from the Community Fault Model 5.2 (Plesch *et al.*, 2007, Nicholson *et al.*, 2017) between 3.5 and 2.5 km in depth. The resolution of controlling points is about 3km and we focus on first-order macroscopic geometric complexities in the fault system. Spatial resolution of the mesh on the fault is about 200 m. Notations: SJF, San Jacinto Fault Claremont segment; CLCZ-CHLM, Cholame segment; CLCZ-CRRZ, Carrizo segment; MJVS, Mojave segment; MULT1, Indo segment; PARK, Parkfield segment; SBMT-SAF, San Bernardino segment.

In terms of rupture extents, we find several representative events that emerge in the earthquake sequence from the models that produce results comparable to paleoseismological events and may be indicative for future rupture scenarios as shown in Figure 2. Figure 2a shows a super-large rupture that has the extent similar to the 1857 Fort Tejon earthquake. Figure 2b show a large rupture that breaks the Parkfield and Cholame segments and a major portion of Carrizo segment. Figure 2c shows a rupture that has a similar rupture extent to the 1812 earthquake. Figure 2d and 2e show earthquakes like the 1899, 1918 and 1923 earthquake sequence occurred on the San Jacinto fault. Figure 2f and 2h show super-large ruptures that nucleate near the Cajon Pass and propagate through the whole fault system. The event in 2h involves a rupture that jumps from the San Jacinto fault over the Cajon Pass to the San Andreas fault. This event suggest ruptures that nucleate on the San Jacinto Fault can occasionally jump over the Cajon Pass earthquake gate and break the Mojave and the San Bernardino segment. Such ruptures that go through the earthquake gate are important in assessing the seismic hazard along the fault system.

The Big Bend, a restraining bend where ~ 40˚ change in fault strikes occurs, is typically a very strong barrier to earthquake ruptures based on empirical relations from fault maps (Biasi and Wesnousky, 2017) and inferences from paleoseismicity (Scharer *et al.*, 2014). Our results show the Big Bend is indeed such a barrier. Ruptures tend to naturally stop at the Big Bend as shown by Figure 2b and 2c. Ruptures that break the Big Bend in our models typically involve triggering by seismic waves tens of kilometers over the Big Bend. Ruptures from the south tend to go through the Big Bend easier than ruptures from the north.

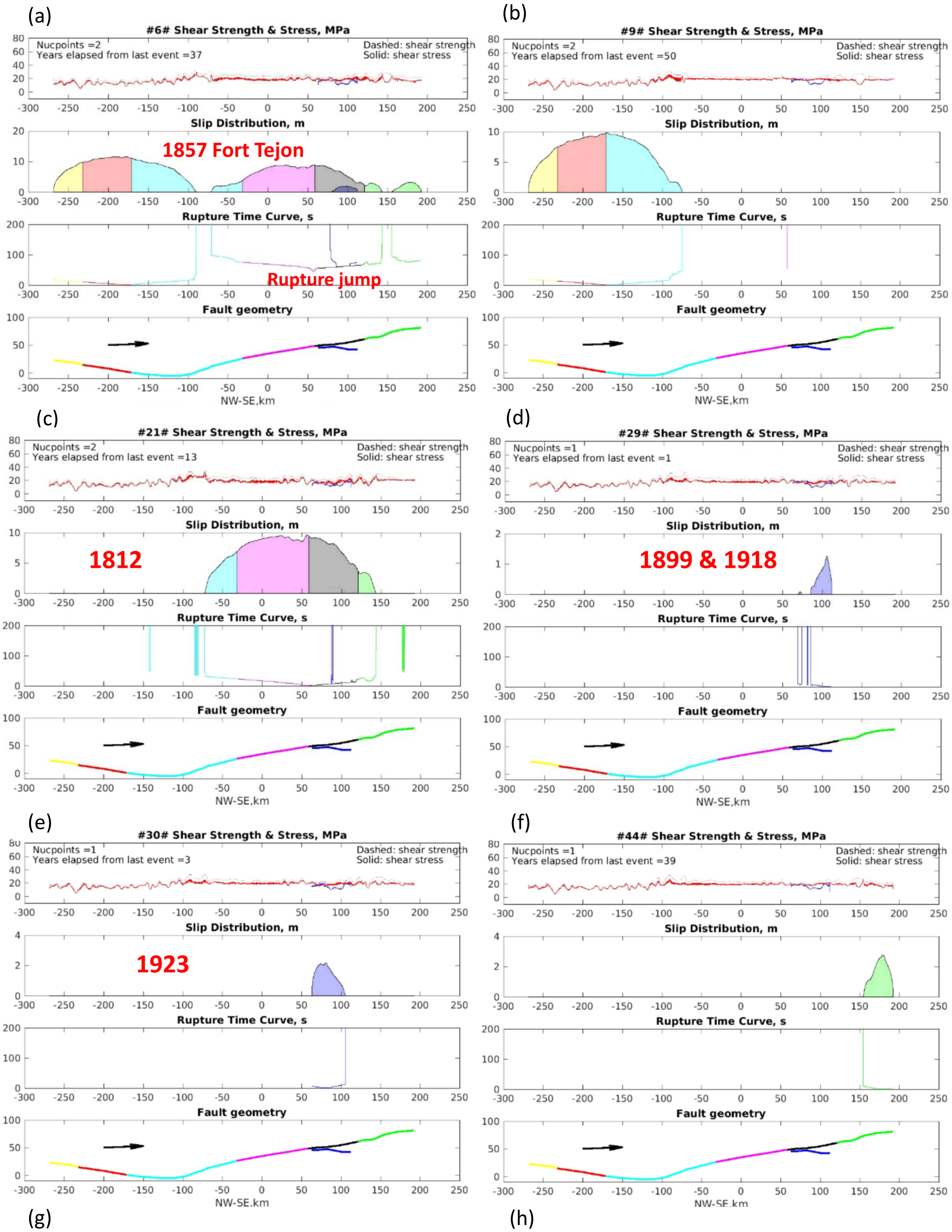
(a)
#6# Shear Strength & Stress, MPa
Nucpoints =2
Years elapsed from last event =37
Dashed: shear strength
Solid: shear stress
Slip Distribution, m
1857 Fort Tejon
Rupture Time Curve, s
Rupture jump
Fault geometry
NW-SE,km
(b)
#9# Shear Strength & Stress, MPa
Nucpoints =2
Years elapsed from last event =50
Dashed: shear strength
Solid: shear stress
Slip Distribution, m
Rupture Time Curve, s
Fault geometry
NW-SE,km
(c)
#21# Shear Strength & Stress, MPa
Nucpoints =2
Years elapsed from last event =13
Dashed: shear strength
Solid: shear stress
Slip Distribution, m
1812
Rupture Time Curve, s
Fault geometry
NW-SE,km
(d)
#29# Shear Strength & Stress, MPa
Nucpoints =1
Years elapsed from last event =1
Dashed: shear strength
Solid: shear stress
Slip Distribution, m
1899 & 1918
Rupture Time Curve, s
Fault geometry
NW-SE,km
(e)
#30# Shear Strength & Stress, MPa
Nucpoints =1
Years elapsed from last event =3
Dashed: shear strength
Solid: shear stress
Slip Distribution, m
1923
Rupture Time Curve, s
Fault geometry
NW-SE,km
(f)
#44# Shear Strength & Stress, MPa
Nucpoints =1
Years elapsed from last event =39
Dashed: shear strength
Solid: shear stress
Slip Distribution, m
Rupture Time Curve, s
Fault geometry
NW-SE,km
(g)
(h)

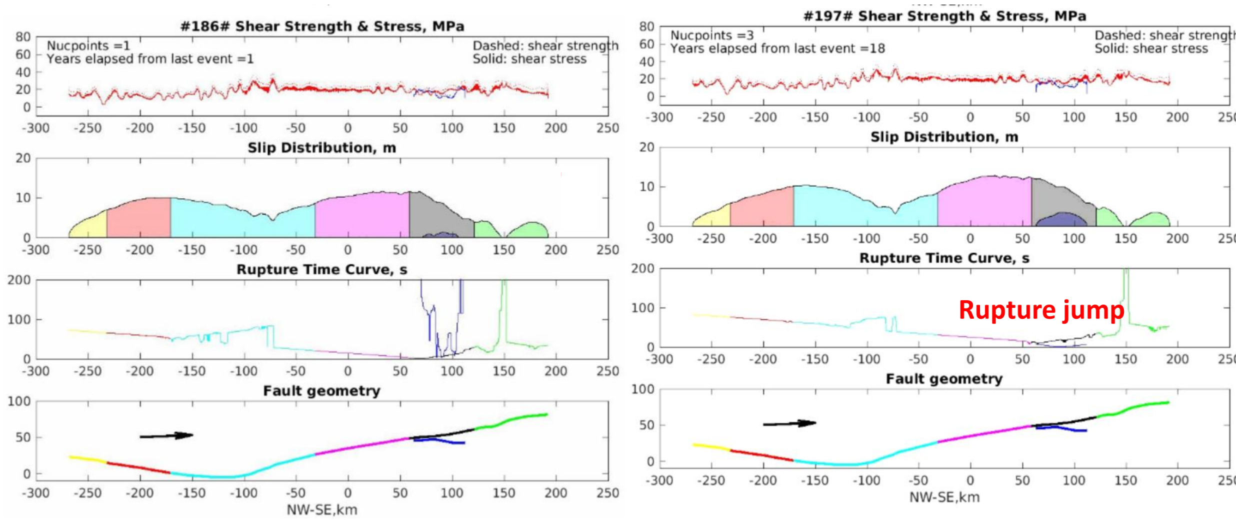

Figure 2. Representative rupture scenarios from the earthquake sequence simulated. (a) A super-large rupture that breaks the whole fault system, which shows potential like the 1857 Fort Tejon earthquake. (b) A large rupture that breaks the San Andreas segments northwest to the Big Bend. (c) A large rupture that breaks most of the San Andreas segments southeast to the Big Bend. (d-e) Moderate earthquakes occurring on the San Jacinto fault that are comparable to 1899, 1918, 1923 earthquakes. (f) A moderate earthquake that breaks the Indo segment. (g-h) Super-large ruptures that nucleate near the Cajon Pass and break the whole fault system, in which event h involves the rupture jump from the San Jacinto fault over the Cajon Pass to the San Andreas fault.

References cited in this report:

Biasi, G.P. & Wesnousky, S.G., 2017. Bends and Ends of Surface Ruptures, *Bull. Seismol. Soc. Am.,* 107**,** 2543-2560.

Duan, B., 2019. Multicycle Dynamics of the Aksay Bend Along the Altyn Tagh Fault in Northwest China: 1. A Simplified Double Bend, *Tectonics*.

Duan, B., Liu, Z. & Elliott, A.J., 2019. Multicycle Dynamics of the Aksay Bend Along the Altyn Tagh Fault in Northwest China: 2. The Realistically Complex Fault Geometry, *Tectonics*.

Duan, B. & Oglesby, D.D., 2005. Multicycle dynamics of nonplanar strike-slip faults, *Journal of Geophysical Research: Solid Earth (1978–2012),* 110.

Nicholson, C., Plesch, A. & Shaw, J., 2017. Community Fault Model Version 5.2: Updating & expanding the CFM 3D fault set and its associated fault database. *in Poster Presentation at 2017 Southern California Earthquake Center (SCEC) Annual Meeting*.

Plesch, A., Shaw, J.H., Benson, C., Bryant, W.A., Carena, S., Cooke, M., Dolan, J., Fuis, G., Gath, E., Grant, L., Hauksson, E., Jordan, T., Kamerling, M., Legg, M., Lindvall, S., Magistrale, H., Nicholson, C., Niemi, N., Oskin, M., Perry, S., Planansky, G., Rockwell, T., Shearer, P., Sorlien, C., Süss, M.P., Suppe, J., Treiman, J. & Yeats, R., 2007. Community Fault Model (CFM) for Southern California, *Bull. Seismol. Soc. Am.,* 97**,** 1793-1802.

Scharer, K., Weldon, R., Streig, A. & Fumal, T., 2014. Paleoearthquakes at Frazier Mountain, California delimit extent and frequency of past San Andreas Fault ruptures along 1857 trace, *Geophys. Res. Lett.,* 41**,** 4527-4534.